Research Square

Preprints are preliminary reports that have not undergone peer review.
They should not be considered conclusive, used to inform clinical practice,
or referenced by the media as validated information.

Histamine H 3 receptor expression in trigeminal ganglion and migraine-related regions in rat brain

Aida Maddahi

Aida.maddahi@med.lu.se

Lund University Hospital

Lanfranco Pellesi

University of Southern Denmark

Lars Edvinsson

Lund University Hospital

Research Article

Keywords: Calcitonin gene-related peptide, histamine, headache, migraine, pain, trigeminal ganglion

Posted Date: November 25th, 2026

DOI: https://doi.org/10.21203/rs.3.rs-11772344/v1

License: This work is licensed under a Creative Commons Attribution 4.0 International License.
Read Full License

Additional Declarations: No competing interests reported.

Histamine H_3 receptor expression in trigeminal ganglion and migraine-related regions in rat brain

Aida Maddahi[1*], Lanfranco Pellesi[2] and Lars Edvinsson[1]

[1]Division of Experimental Vascular Research, Department of Clinical Sciences, Lund University Hospital, Lund, Sweden

[2]Department of Public Health, Clinical Pharmacology, Pharmacy and Environmental Medicine, University of Southern Denmark, Campusvej 55, 5230 Odense, Denmark

*Corresponding author:

Aida Maddahi, PhD
Department of Clinical Sciences,
Division of Experimental Vascular Research,
BMC A13, Sölvegatan 17, SE-221 84, Lund, Sweden
Aida.maddahi@med.lu.se

Abstract

Background: Migraine is a complex neurological disorder involving activation of the trigeminovascular system (TVS), in which calcitonin gene-related peptide (CGRP) plays an important role in pain signaling. Histamine has been associated with migraine, however, histamine H_1 and H_2 receptors antagonism has not been effective. Recent evidence of histamine H_3 receptor (H3R) involvement in neurotransmitter regulation has generated interest in its potential role in migraine. The distribution of H3R in migraine-related brain regions and in the trigeminal system have not been thoroughly investigated. Therefore, the aim of the present study was to examine H3R expression in migraine-related brain regions, trigeminal ganglion (TG), sphenopalatine ganglion (SPG) and dorsal root ganglion (DRG), as well as its co-localization with CGRP in the TG.

Methods: The TG, SPG, DRG, basilar artery, brain and hypothalamus were dissected from adult male rats. RT-qPCR and immunohistochemistry were used to assess the mRNA and protein expression for H3R.

Results: Immunohistochemical analysis showed H3R immunoreactivity in migraine-related brain regions and peripheral ganglia. H3R showed a similar expression pattern in the TG, SPG and DRG. H3R immunoreactivity was detected mainly in the nuclei, with some staining also observed in the cytoplasm of neurons, satellite glial cells (SGCs) and fibers. H3R showed co-localized with CGRP in small to medium sized neurons in the TG. RT-qPCR analysis showed significantly higher H3R mRNA levels in the hypothalamus compared with the TG. In cerebral arteries, H3R immunoreactivity was mainly localized in endothelial cells.

Conclusions: H3R is widely expressed in several migraine-related brain regions as well as in peripheral ganglia and cranial arteries. The co-localization of H3R with CGRP in TG indicates

a possible interaction between H3R and the CGRP peptide, supporting further investigation of H3R in migraine pathophysiology.

Keywords: Calcitonin gene-related peptide, histamine, headache, migraine, pain, trigeminal ganglion.

Background

Migraine is a chronic, painful and complex neurological disorder which affects up to 15% of the world's population. It is characterized by recurrent attacks of headache, unilateral and pulsating, often aggravated by physical activity and accompanied by nausea, vomiting, photophobia and phonophobia [1-3]. The mechanisms underlying migraine are complex and involve both peripheral and central components of the nervous system. Activation of the trigeminovascular system (TVS) has an important role in migraine pain, and calcitonin gene-related peptide (CGRP) being one of the neurotransmitters involved in peripheral and central pain signaling [4]. CGRP and its canonical receptors are widely expressed within the trigeminal system which supports an important role for CGRP signaling in trigeminal sensory pathways [4, 5].

Histamine is a neurotransmitter and inflammatory mediator involved in several physiological processes [6] and has long been associated with headache and migraine [7]. Previous studies showed that administration of histamine can induce headache [8-10] supporting a potential role of histaminergic signaling in migraine [7]. Histamine exerts its effects through four G protein-coupled receptors, H_1, H_2, H_3 and H_4. Among these, the histamine H_3 receptor (H3R) is of particular interest because of its expression in the central nervous system (CNS) and its role in regulating neurotransmitter release [11-13].

The H3R acts as a presynaptic auto-receptor on histaminergic neurons. H3R activation inhibits histamine release through a negative feedback mechanism [11]. H3R can also act as a heteroreceptor on other neuronal populations, modulating the release of several neurotransmitters, suggestive of a broader role in neuronal signaling [12, 13]. Autoradiographic studies have demonstrated a widespread but regionally variable distribution of H3R in the rat brain [14]. Recently, the possible involvement of H3R in migraine has gained

interest and modulation of H3R signaling is currently being investigated in individuals with migraine [15].

Studying H3R expressions in migraine-related brain regions may help clarify its role in migraine mechanisms. Moreover, investigating the relationship between H3R and CGRP may provide further insights into the involvement of H3R in trigeminal signaling.

The aim of the present study was to investigate the expression and distribution of H3R in peripheral ganglia, including the trigeminal ganglion (TG), sphenopalatine ganglion (SPG) and dorsal root ganglion (DRG), as well as in the cerebral artery and brain regions involved in migraine, using RT-qPCR and immunohistochemistry. In addition, we examined the co-localization of H3R with CGRP in the TG.

Experimental procedures

Animals

All animal procedures in this study followed the guidelines of the European Communities Council (86/609/ECC) and were approved by the Regional Ethical Committee on Animal Research at the University of Lund, Sweden (LU-818-01). The animals were housed under controlled temperature and humidity with free access to water and food ad libitum and were kept under a 12:12-hour light: dark cycle (lights on at 10:00 a.m.).

Tissue preparation

A total of 14 male Wistar rats, weighing approximately 250-300 g, were used for immunohistochemistry and RT-qPCR analysis. All animals were anaesthetized using CO_2 and killed by decapitation. Brain, TGs, SPG (right and left), DRG, basilar artery (BA) and hypothalamus (HT) were carefully dissected. The brains were cut sagittal in the midline. For

immunohistochemistry, the brains, SPGs, TGs, DRGs and BA were fixed in 4% paraformaldehyde (PF) in phosphate buffer saline (PBS, Sigma Aldrich, pH 7.2) overnight at 4°C. Thereafter, all fixed tissues were cryo-protected with Sörensen's phosphate buffer (pH 7.2) gradient containing 10% and 25% sucrose overnight. Then they were embedded in an egg albumin-based protein medium or in Tissue Tek (O.C.T. Compound, Sakura, Poland) and sectioned at a thickness of 10 µm using a cryostat (Microm Cryo Star HM 560). Finally, the sections were collected on microscope slides (Superfrost^{TM,} Merck Chemicals and Life Science, Sweden) and stored at -20 ºC until use. For RT-qPCR, the TGs (left and right from each rat), and hypothalamus were dissected and immediately fresh frozen in liquid nitrogen. Then they were collected in a 2 ml Eppendorf tube and stored at -80 ºC for further analysis.

RNA isolation and RT-qPCR

A total of 8 rats were used for RT-qPCR. The HT and TGs (both left and right) were carefully dissected and immediately frozen in liquid nitrogen for RNA extraction. All RNA extraction was performed using RNeasy® Plus Mini kit (Qiagen, Hilden, Germany) in accordance with the manufacturer's protocol. Total RNA concentration was determined using a GeneQuant Pro spectrophotometer (Amersham Pharmacia Biotech, Uppsala, Sweden). A ratio of sample absorbance at 260/280 nm in the range of 1.8 to 2 was considered acceptable. First-strand cDNA was prepared from 1 µg of total RNA (from TG and hypothalamus) in a 20 µL reverse transcript reaction using Superscript® III First-Strand Synthesis Super Mix (Invitrogen, Carlsbad, CA, USA). A reverse transcription negative control to detect the genomic DNA was performed simultaneously for each sample and underwent the same procedures but without Superscript III Reverse Transcriptase (RT enzyme). The cDNA obtained was diluted to a total volume of 80 µL and stored at -20°C. The primer sequences were specific for the genes of interest and were designed for Rattus norvegicus, using Primer Express 3.0 software (PE

Applied Biosystems, Foster city, CA, USA), and synthesized by TAG Copenhagen A/S (Copenhagen, Denmark). The housekeeping gene glyceraldehyde-3-phosphate dehydrogenase (GAPDH) was used as a reference gene, and the gene expressions were normalized versus that gene. Primers had the following sequences:

HRH3, NM 053506 (forward; 5`- TACTGTGTGCCTCCTCGGTCTT -3`, revers; 5` - AGCTCGAGTGACTGACAGGAATC -3`) and GAPDH (forward; 5`- CTGCACCACCAACTGCTTAGG -3`, revers; 5´-TCAGCTCTGGGATGACCTTGC- 3`).

The RT-qPCR was performed in 20 µL reaction consisting of 2 µL diluted cDNA, 0.5 µM of each primer, 10 µL Fast SYBR™ Green Master Mix (Applied Biosystems, CA, USA), and 7 µL RNase free water in a Step One Plus Real Time PCR System (Applied Biosystems, CA, USA) with the following thermal profile: Holding stage at +50°C for 2 min, +95°C for 10 min, followed by 40 PCR cycles at +95°C for 15 s and +60°C for 1 min. Each sample was examined in duplicate, and a blank control (without template) was used in all experiments. After amplification a melting curve analysis was performed to confirm specificity of primers annealing and to verify that each primer pair generated only one PCR product of expected size.

Immunohistochemistry

Sections of TG, SPG, DRG and BA obtained from six male rats were washed and permeabilized in PBS containing 0.3% Triton X-100 (PBST) for 20 min. Thereafter, the tissue sections were blocked for 1 h at room temperature in a blocking solution containing PBST, 1% bovine serum albumin (BSA), and 5% normal serum to reduce non-specific antibody binding. The sections were then incubated overnight at 4°C in humidified chambers with primary antibodies (for antibody details, see Table 1).

The following day, the sections were washed three times for 15 min each in PBST and incubated with the appropriate secondary antibodies (for details, see Table 1) for 1 h at room temperature in the dark to minimize photobleaching. All antibodies were diluted in PBST containing 1% BSA. The sections were subsequently washed three times for 15 min each in PBST and mounted with Vectashield antifade mounting medium containing 4′,6-diamidino-2-phenylindole (DAPI) (Vector Laboratories, Burlingame, CA, USA).

Table 1. Primary and secondary antibodies are used for immunohistochemistry

Primary antibodies

Name and product code	Dilution	Host	Supplier
CGRP (ab81887)	1:100	Mouse	Abcam, Cambridge, UK
H3R (AHR-003)	1:200	Rabbit	Alomone Labs, Jerusalem, Israel
H3R(ab317387)	1:200	Rabbit	Abcam, Cambridge, UK
H3R (LS-C383932)	1:100	Mouse	LSBio, Newark, CA

Secondary antibodies

Name	Dilution	Against	Supplier
Alexa 594	1:200	Mouse	Thermo Scientific, IL, USA
Alexa 488	1:100	Rabbit	Thermo Scientific, IL, USA

Negative controls were performed by omitting the primary antibodies to assess tissue autofluorescence and non-specific binding of the secondary antibodies. Immunoreactivity was visualized using an epifluorescence microscope (Nikon 80i; Tokyo, Japan) at the appropriate excitation and emission wavelengths, and images were acquired using an attached Nikon DS-

2Mv camera. Images were processed using Adobe Photoshop CS3 (Adobe Systems, Mountain View, CA, USA).

To further validate H3R immunoreactivity, three different antibodies from independent suppliers (Alomone Labs, Abcam, and LifeSpan BioSciences) were used to detect H3R expressions.

Furthermore, a pre-absorption control (blocking peptide control) was performed to confirm the specificity of the AHR-003 antibody (Alomone Labs). Briefly, the primary antibody was mixed with the corresponding blocking peptide (BLP-HR003) at a ratio of 1 µg peptide per 1 µg antibody and incubated for 1 h at room temperature. Following incubation, the antibody-peptide mixture was applied to the tissue sections and the immunohistochemical staining procedure was continued as described above.

Double immunohistochemistry was performed to examine H3R and CGRP co-localization in TG tissue. The primary antibodies against H3R and CGRP were mixed and applied simultaneously as an antibody cocktail. The remaining staining procedure was performed as described above.

Calculation and statistical analyses

RT-qPCR data were analyzed with the comparative cycle threshold (C) method [16]. Fold change and standard deviations were calculated using the ΔCT method.

Statistical analysis was performed using Graph Pad Prism 9. Statistical significance was determined using Mann-Whitney or Student's T-test. Data were expressed as mean ± standard error of the mean (SEM), *n* refers to the number of rats, $^{**}P < 0.01$ was considered significant.

Results

Gene expressions of H3R in TG and hypothalamus

Expression of the H3R gene in TG and HT was determined by real-time PCR analysis of tissue mRNA. In each qPCR experiment, either a no template control (NTC, water control) or a minus RT control was included and there were no signs of contamination, primer-dimer and/or genomic DNA in the samples. The expression of the house keeping gene GAPDH was used to normalize gene expression.

The results in Figure 1 showed that H3R gene was expressed in both TG and HT, however the mRNA level for H3R was significantly higher in the HT compared to the TG.

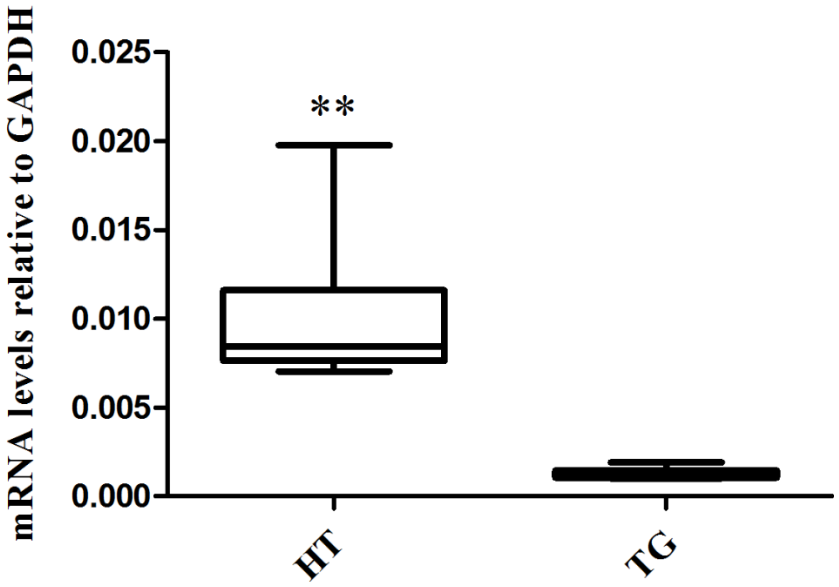

Immunohistochemistry

Specificity of H3R antibody with blocking peptide

There were no staining and/or H3R immunoreactivity with pre-absorbed H3R antibody when using its blocking peptide (Fig. 2). This shows the specificity of H3R antibody.

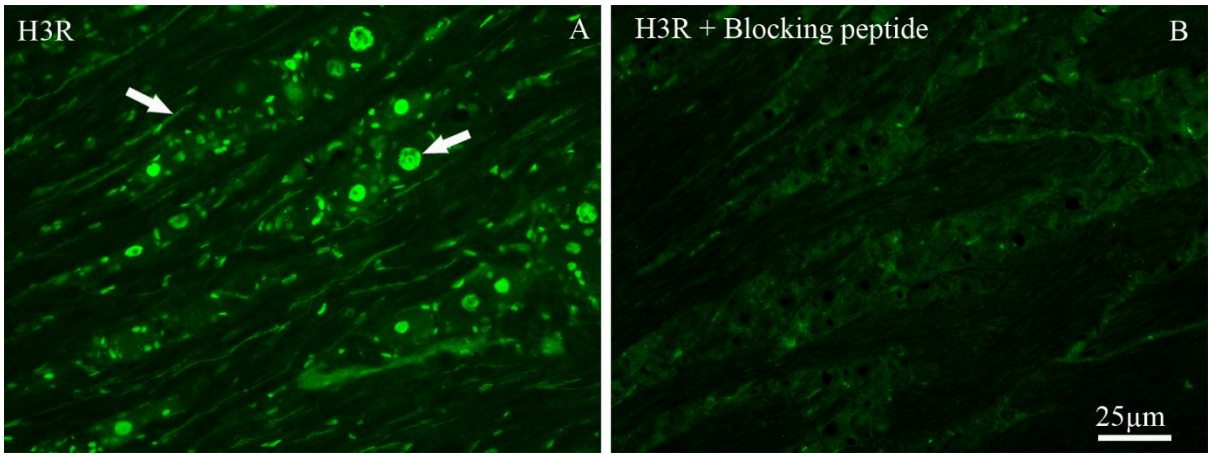

Distribution of H3R in the TG, SPG and DRG

To confirm H3R expression in the TG, SPG and DRG, we tested three H3R antibodies from three different companies: (1) a rabbit polyclonal anti-HRH3 antibody (AHR-003; Alomone Labs), (2) a rabbit monoclonal anti-HRH3 antibody [S04-3I4] (ab317387; Abcam), and (3) a rabbit polyclonal anti-HRH3 antibody (LS-C383932; LSBio).

Overall, all three antibodies showed similar patterns of H3R immunoreactivity, although differences were observed in staining intensity and subcellular localization. The AHR-003 antibody produced clear H3R staining in the nuclei of TG neurons of various sizes and in the satellite glial cells (SGCs), as well as in fibers. Nuclear staining was markedly stronger than the staining observed in the fibers (Fig. 3).

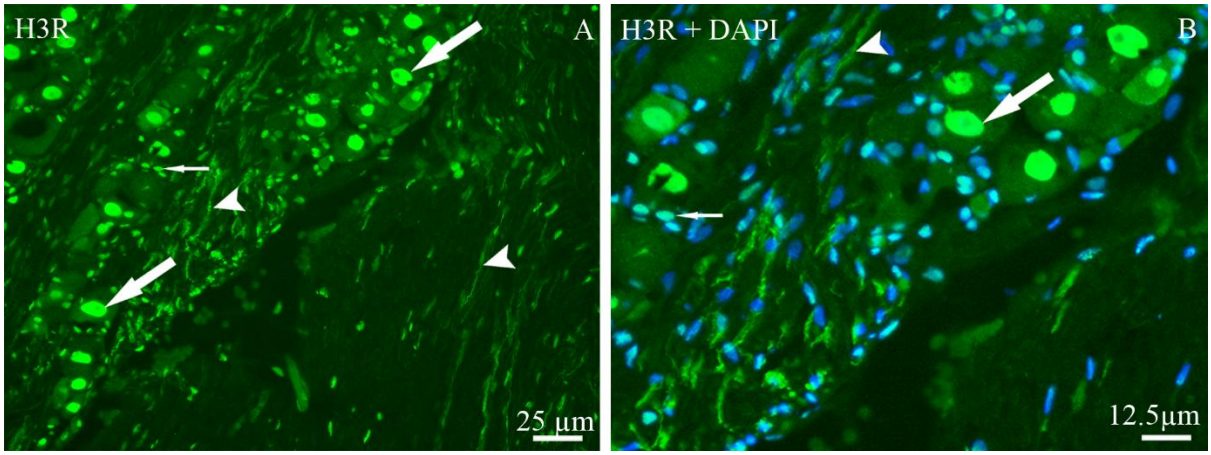

A similar pattern was observed with the Abcam antibody, which showed predominant nuclear staining in TG neurons and some cytoplasmic staining in medium to large-sized neurons and SGCs. Strong H3R immunoreactivity was also detected in fibers (Supplementary Fig. 1). The LSBio antibody likewise showed H3R immunoreactivity in both the nuclei and cytoplasm of TG neurons with a weaker expression in the fibers.

Since all three antibodies consistently demonstrated nuclear H3R immunoreactivity and the specificity of AHR-003 staining was further validated by pre-absorption experiments, AHR-003 was selected for representative staining in the images presented in this study. This choice was additionally supported by its well documented use in published literature.

Expression of H3R was also examined in other sensory ganglia involved in pain pathology, the DRG and SPG. As shown in Figure 4, similar distribution pattern of H3R immunoreactivity was observed in the SPG and DRG. Staining was detected in the nuclei of neurons and SGCs, as well as in the fibers.

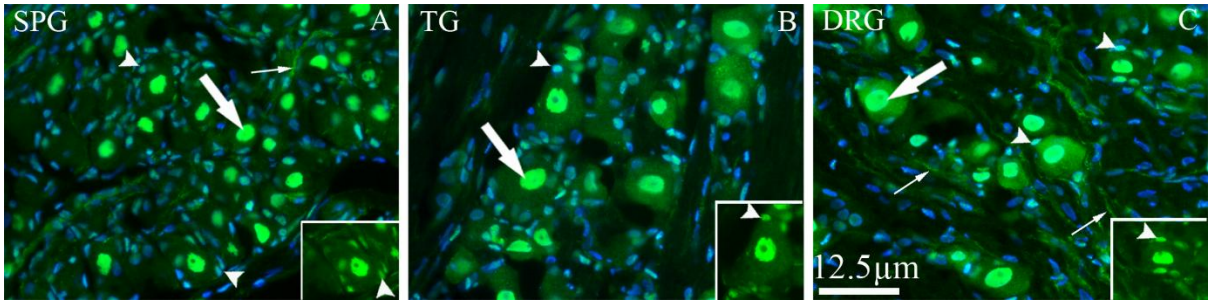

Co-localization of H3R with CGRP in the TG

We examined the expression of H3R in relation to CGRP in the TG using both H3R antibodies from Alomone and Abcam. With the Alomone antibody, H3R and CGRP were detected in the same small to medium-sized neurons. H3R staining was mainly observed in the nuclei, whereas CGRP staining was present in the cytoplasm (Fig. 5A-C). Thus, the two proteins were co-expressed in the same neurons but did not show clear co-localization. CGRP immunoreactivity was also observed in thin nerve fibers (C-fibers) (Fig. 5B).

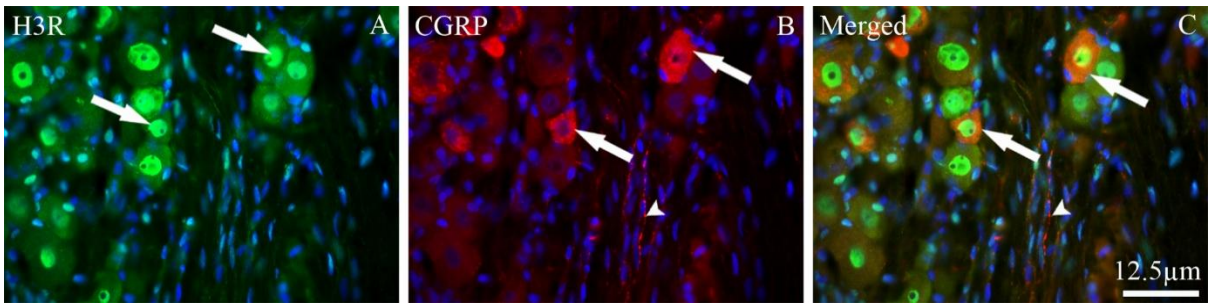

With the Abcam antibody, H3R and CGRP showed clear co-localization in the cytoplasm of some small to medium-sized neurons, visible as overlapping yellow/orange staining in the merged image (Supplementary Fig. 2). H3R immunoreactivity was mainly observed in thicker nerve fibers, but a weaker H3R staining and some overlap with CGRP were also seen in thin fibers.

Distribution of H3R in the brain related to migraine area

The results of our H3R mapping study are summarized in Fig.6. We compared the brain regions identified in human imaging studies during migraine attacks [17] with the distribution of CGRP observed in our previous study [18] and H3R immunoreactivity identified in the present study (Fig. 6).

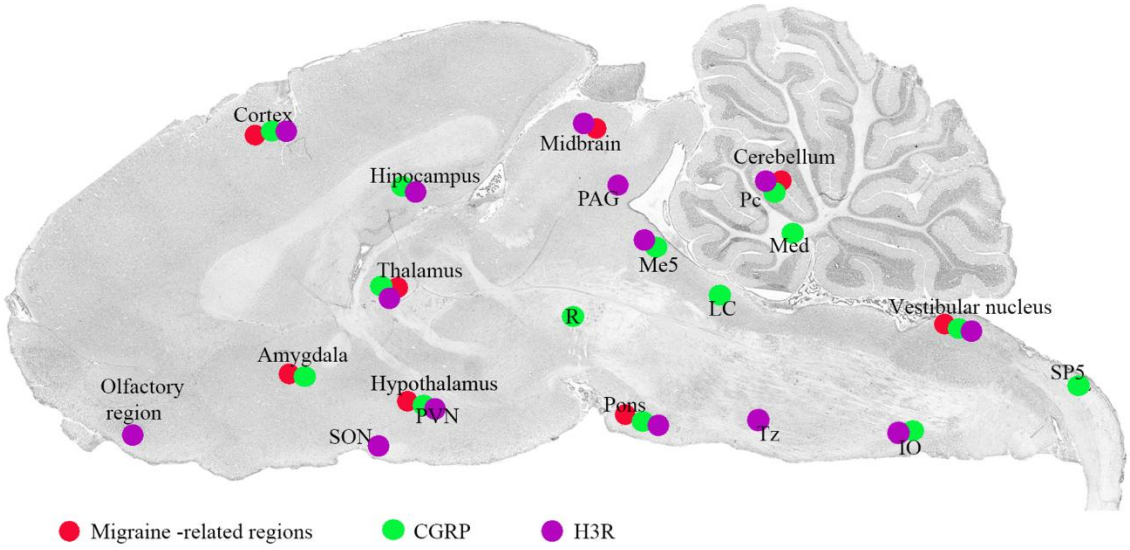

Brainstem and medulla oblongata

In the pons, H3R expression was observed in the pontine nuclei (Pn), the pontine reticular nucleus (PnO), and the transverse fibers of the pons (tfP) (Fig. 7A). At higher magnification (Fig. 7B), H3R protein was localized in both the cytoplasm and nuclei of neurons within these regions and some in the fibers.

In addition, in the pontine region of the brainstem, the nuclei of the trapezoid body (Tz) also showed H3R immunoreactivity (Fig.7C). H3R immunoreactivity was observed in cell body of neurons within the Tz together with immunoreactive fibers distributed throughout the surrounding neuropil.

The inferior olivary nucleus (ION), located in the medulla oblongata, plays an important role in motor coordination by transmitting signals to the cerebellum [32]. H3R immunoreactivity was detected in neurons and fibers of the IO (7D).

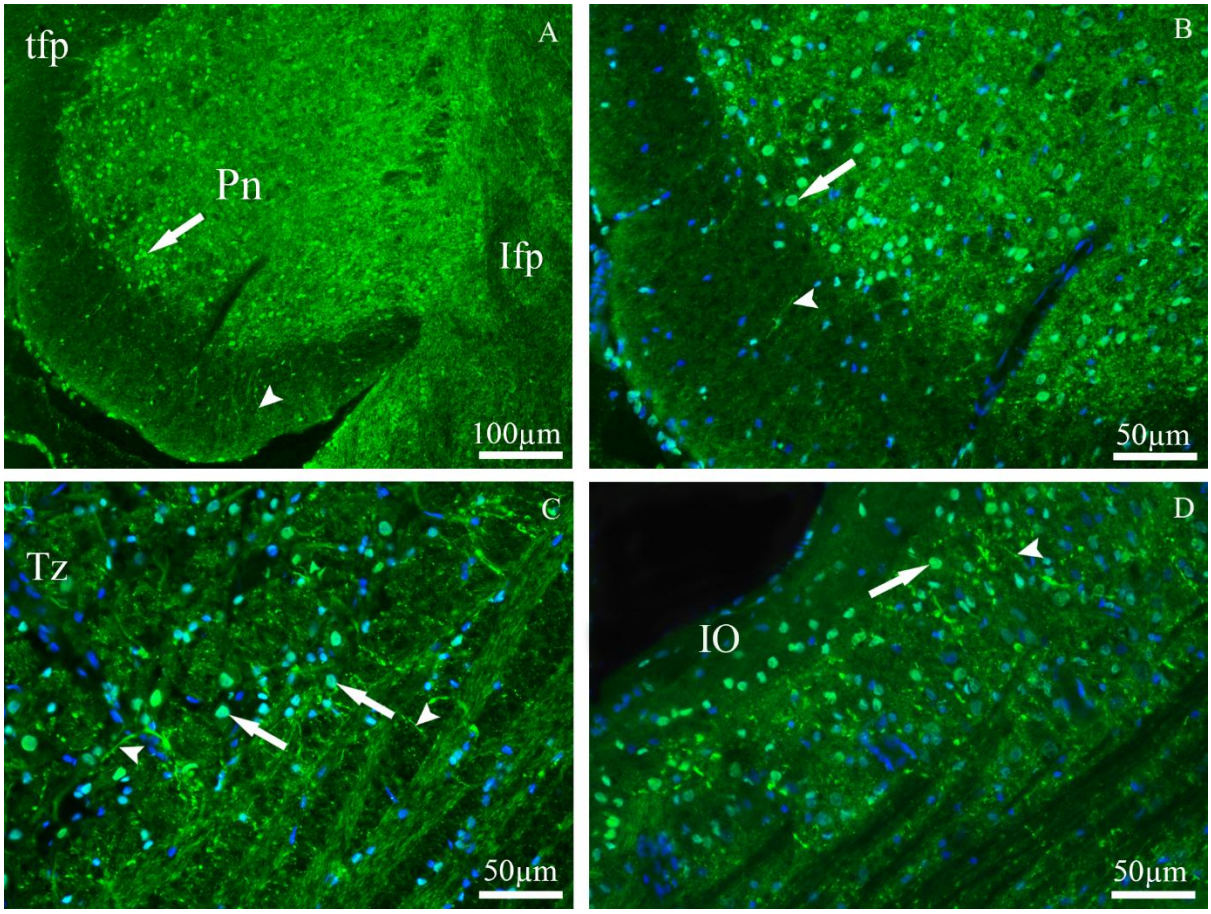

Further, H3R expressions were detected in several nuclei of the dorsal brainstem, with a distinct regional distribution. As shown in Figure 8 A, H3R immunoreactivity was present in the nucleus of the solitary tract (Sol), the cuneate nucleus (cu), and the external cuneate nucleus (Ecu). The H3R immunoreactivity was strong in Sol, where a dense H3R staining was seen not only in cellular profiles but also in numerous fibers forming a dense network throughout the region (Fig. 8B and C). In comparison, the cu showed weaker and less extensive staining. H3R immunoreactivity was also observed in the Ecu, although it seems less pronounced than in the Sol. This indicates H3R expression across multiple sensory related brainstem nuclei.

The Medial vestibular nucleus (MVe) is located in the dorsolateral medulla and caudal pons, and H3R immunoreactivity was observed in the cell bodies (somata) of neurons within the Mve, as well as in the surrounding neuropil and fibers (Fig.8D).

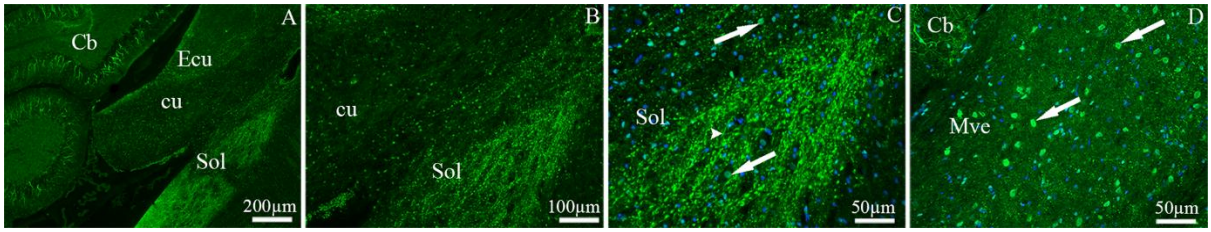

Cerebellum

The cerebellar cortex is composed of three layers: the granule cell layer, which is located adjacent to the white matter; the molecular layer, which is located at the surface of the cerebellum; and the Purkinje cell (PC) layer, which is located between these two layers and consists mainly of a monolayer large Purkinje cell bodies.

H3R immunoreactivity was observed in the cerebellar cortex, especially in the Purkinje cell and molecular layers (Fig. 9A). The H3R immunoreactivity was found in the cell body of Purkinje cells, while numerous dendritic processes extended from the cell bodies into the molecular layer. These dendrites showed strong H3R immunoreactivity and were extensively branched, forming a dense network throughout the molecular layer (Fig. 9A & B).

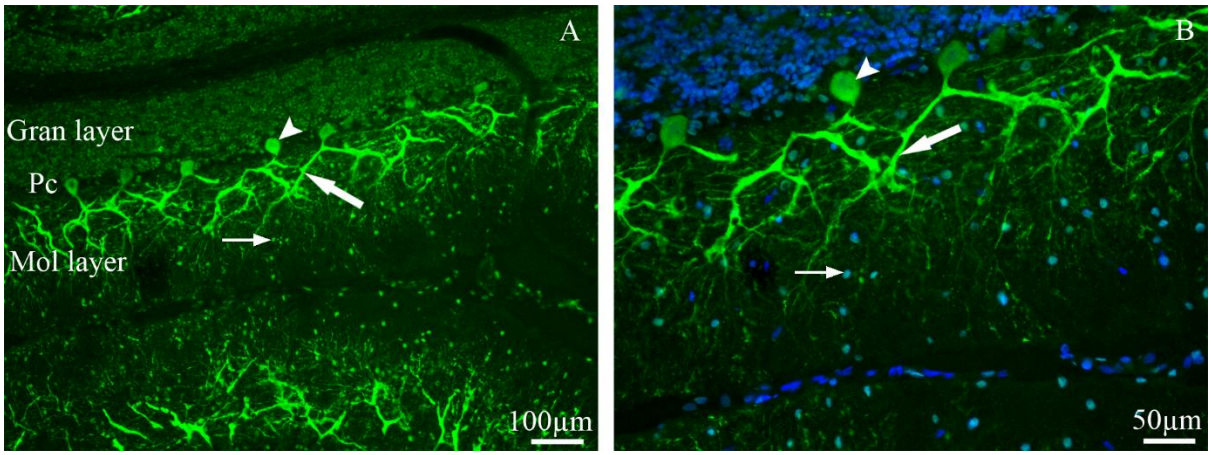

Cerebral cortex

In cerebral cortex, H3R immunoreactivity was detected throughout the cortical layers examined (layers I-V), although the intensity and distribution of H3R expression varied across the cortical depth. The strongest H3R immunoreactivity was observed in layers II, III and IV. The staining appeared as a dense network of immunoreactive neuronal processes and fibers, together with distinct cellular profiles (Fig. 10A). In contrast, layer I showed more diffuse and less intense staining, while the deeper cortical region (layer V) displayed weaker and more sparsely distributed immunoreactivity. At higher magnifications, H3R immunoreactivity was observed in both neuronal cell bodies and their processes (Fig.10 C). The cell bodies showed distinct granular staining, while numerous elongated, vertically oriented immunoreactive profiles extended across the cortical layers. These fibers and processes formed a dense network within the cortical neuropil. The strong fiber staining contributed to the H3R immunoreactivity observed in the cortex.

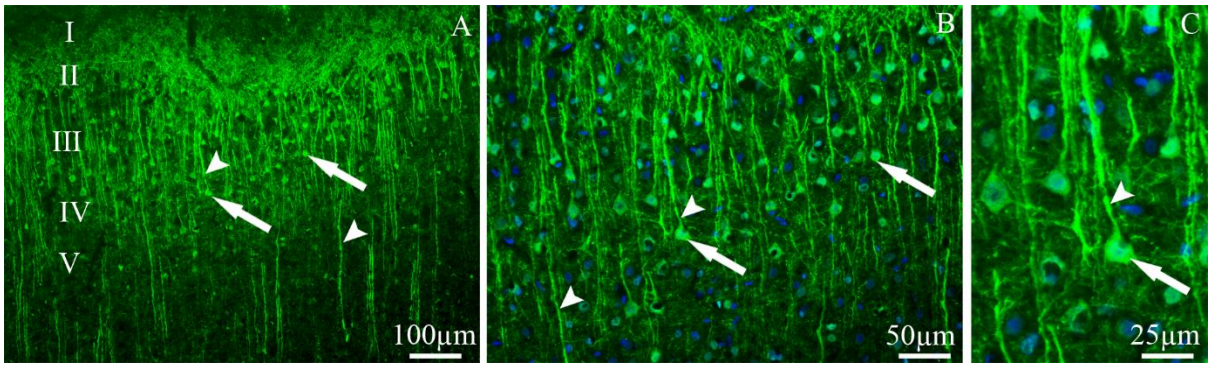

Midbrain

Inferior colliculus (IC) in the midbrain is divided into three main subdivisions: the central nucleus (CIC), the dorsal cortex (DCIC) and the external cortex (ECIC). Immunoreactivity for H3R was observed in the neuronal cell bodies of the IC with a predominant expression in the

DCIC, also additional immunoreactivity distributed throughout the surrounding neuropils and fibers (Fig.11A).

Periaqueductal gray (PAG*)* is also known as the central gray, and it is located around the cerebral aqueduct in the midbrain. H3R immunoreactivity was detected in neuronal cell bodies within the PAG with staining mainly localized in the nuclei (Fig. 11B).

In addition, H3R immunoreactivity was detected in nuclei within the mesencephalic trigeminal nucleus (Me5), together with diffusing H3R-positive staining in the surrounding neuropils (Fig 11C).

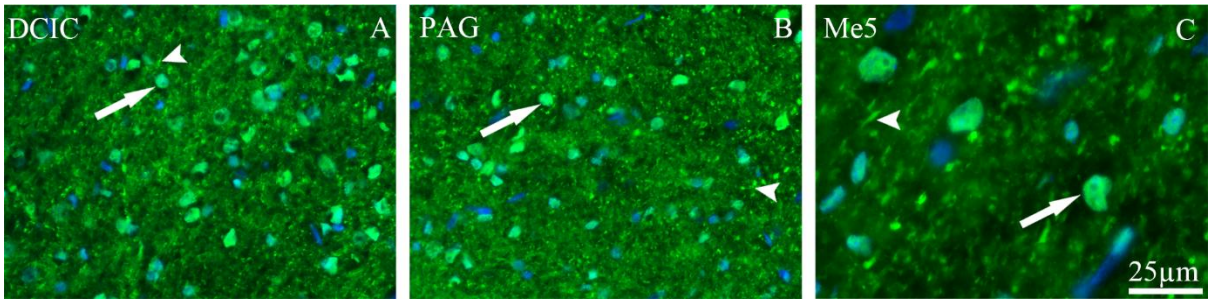

Hippocampus

H3R expression was observed throughout the hippocampus, including the CA1 and CA2 regions and the dentate gyrus (DG) (Fig. 12). The DG showed prominent H3R immunoreactivity, mainly within the densely populated granule cell layer. H3R expression was also detected in pyramidal neurons of the CA1 and CA2 regions, with stronger intensity in CA1 than in CA2. As shown in the higher magnification image of the DG (Fig. 12B), H3R immunoreactivity was strong and widespread throughout the region. Similarly, the higher magnification image of the CA1 region (Fig. 12C) demonstrates H3R expression among neuronal cell bodies within the CA1 area.

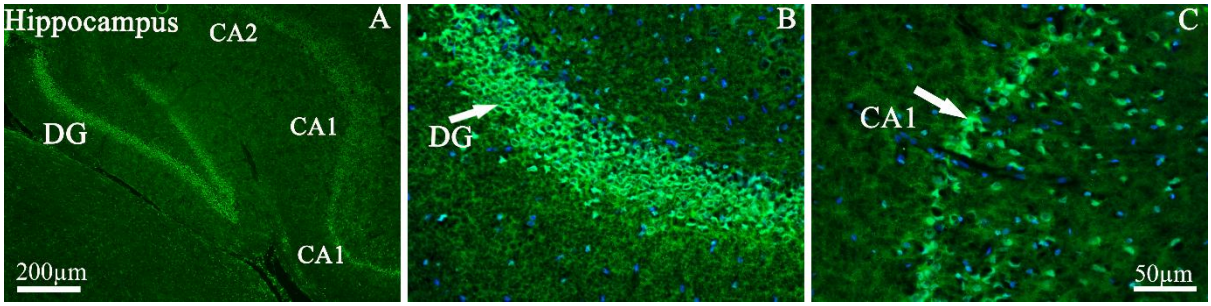

Hypothalamus and thalamus

H3R immunoreactivity was detected in all hypothalamic and thalamic regions examined. The immunoreactive signal appeared as punctate and diffuse green fluorescence within the neuropil and neuronal cells (Fig. 13).

Within the hypothalamus, strong H3R immunoreactivity was observed in both the supraoptic nucleus (SO) (Fig. 13A) and the suprachiasmatic region (SCh) (Fig. 13B). These regions showed similar staining patterns, with some H3R immunoreactivity distributed throughout the areas. The H3R expression was seen in both neuronal somata and the surrounding neuropil and fibers. The H3R expression was also detected in the anterior medial thalamic region (AM) (Fig. 13C), where the staining was less dense and more sparsely distributed than in the SO and SCh regions.

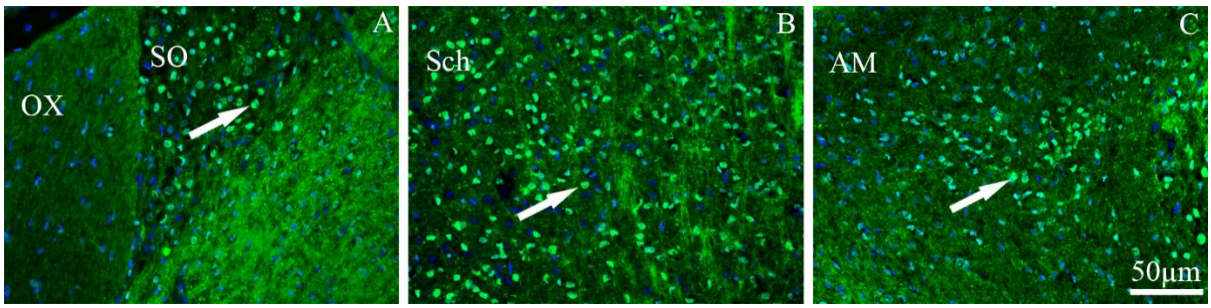

Olfactory area

H3R expression was observed throughout the anterior olfactory nucleus (AON), including the anterior olfactory area (AOV) and anterior olfactory peduncle (AOP) (Fig. 14). The H3R

immunoreactivity was detected within the neuronal cell bodies and their processes. Higher-magnification image (Fig. 14B) showed that H3R was expression in neuronal elements as well as in the fibers within the AON. These observations indicate a strong and widespread distribution of H3R immunoreactivity across both neuronal somatic and process in the anterior olfactory region.

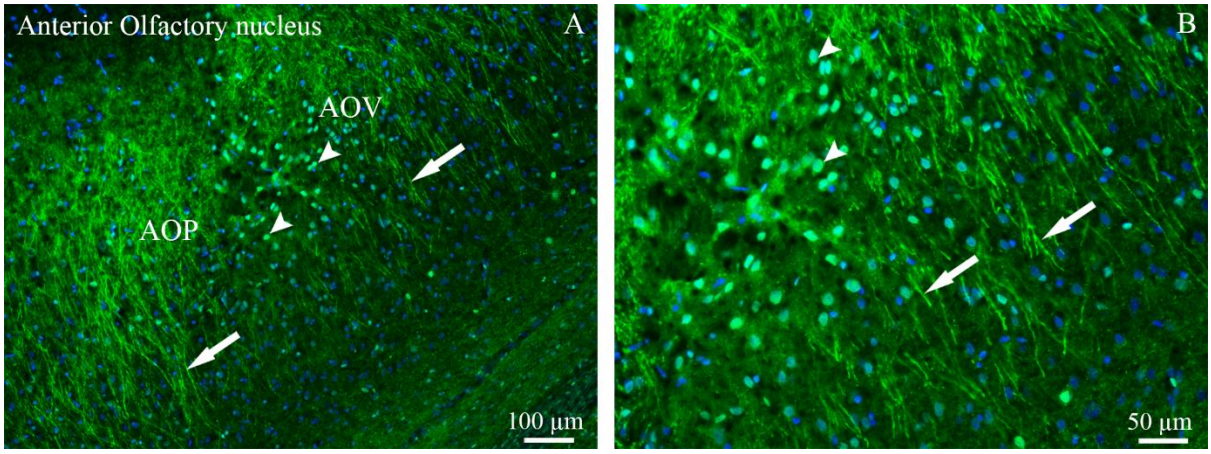

Expression and localization of H3R in cerebral arteries

Cerebral arteries are innervated by trigeminal sensory fibers and constitute a key component of the TVS. Therefore, the potential localization of H3R in the basilar arteries was investigated by immunohistochemistry. Results showed that H3R immunoreactivity was mainly located in the endothelial layer and in some cases, was also detected in the smooth muscle cells (SMCs) in the wall of cerebral arteries (Fig. 15).

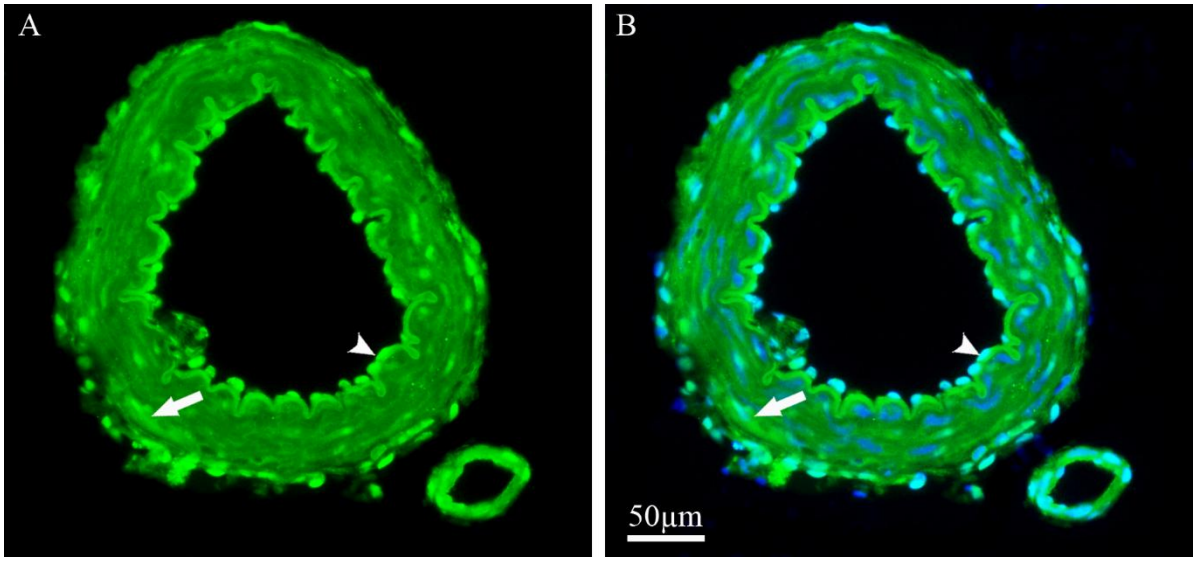

Discussion

The present study investigated the distribution of H3R in central and peripheral structures associated with migraine. H3R immunoreactivity was detected in several migraine-related brain regions including the vestibular nucleus, cerebellum, midbrain, pons, hippocampus, thalamus, hypothalamus and cerebral cortex. In addition, H3R expressions were detected in peripheral structures including the TG, SPG, DRG and cerebral arteries. In the peripheral ganglia, H3R was observed in neurons, SGCs and fibers, with predominantly nuclear staining. In TG, H3R immunoreactivity was found in CGRP-positive neurons and both showing cytoplasmic co-localization when using the Abcam antibody. H3R mRNA was also detected in the hypothalamus and TG, although the expression was significantly higher in the hypothalamus when compared with TG. In the cerebral arteries, H3R immunoreactivity was mainly located in the endothelial cells. Together, these findings provide anatomical evidence for the widespread distribution of H3R in structures relevant to migraine and suggest a possible role for histaminergic signaling in trigeminovascular and autonomic pathways.

H3R distribution in migraine-related brain regions

The widespread distribution of H3R observed in the present study is of interest, as several of these brain regions have previously been associated with migraine. As previously reviewed [19], migraine involves a complex network of central and peripheral structures which include the cerebral cortex, hypothalamus, thalamus and brainstem. The presence of H3R in these regions suggests that histaminergic signaling may contribute to neuronal activity within migraine-related brain areas.

In addition, the widespread H3R immunoreactivity observed in the rat brain agrees with earlier studies investigating H3R distribution in the CNS. Pollard et al. [14] demonstrated extensive H3R binding sites in the rat brain using receptor autoradiography, while Pillot et al. [20] reported H3R mRNA expression and receptor binding in several cortical and subcortical regions. Similarly, Chazot et al. [21] identified H3R immunoreactivity in different regions of the mouse brain. A recent study by Gao et al. [22] reviewed RNA sequencing data showing the expression of several H3R isoforms across different brain regions in humans and mice. More recently, Martins et al. [23] mapped histaminergic pathways in the human brain using transcriptomic and neuroimaging data, providing further evidence for the broad distribution of H3R across cortical and subcortical regions. Overall, all these studies support our findings of H3R immunoreactivity in the cerebral cortex, hypothalamus, thalamus, hippocampus, cerebellum and brainstem. Collectively, the H3R appears to be widely expressed in primary headache related regions.

In the cerebral cortex, we observed H3R immunoreactivity across several cortical layers, mostly layers II-IV and it was located in neuronal cell bodies and processes. This observation is in agreement with a previous study [21], who reported strong H3R mRNA expression in intermediate and deep cortical layers. The widespread cortical expression of H3R is of interest

in relation to migraine, as cortical activity and altered neuronal excitability are important features of the disorder.

H3R immunoreactivity was also observed in several midbrain regions, including the PAG, Me5 and IC. The presence of H3R in the PAG is particularly interesting, as this region plays an important role in pain modulation and has been linked to migraine pathophysiology. Previous imaging studies have reported structural and functional changes in the PAG in patients with migraine [24, 25]. H3R expression was also detected in the Me5, a region mainly involved in proprioceptive processing from the jaw muscles and periodontal tissues [26]. In addition, H3R immunoreactivity was found in the IC, mainly in the dorsal cortex (DCIC). The IC is an important auditory processing center, and the presence of H3R in this region raises the possibility that histaminergic signaling may influence auditory processing and sound sensitivity during migraine attacks [27]. Based on these findings, we believe that H3R may be involved in the regulation of neuronal activity in midbrain pathways associated with pain and sensory processing.

In the hippocampus, H3R staining was observed in the dentate gyrus and CA1-CA2 regions, with staining in neuronal cell bodies and processes. This was in agreement with previous studies [14, 21, 22]. Strong H3R immunoreactivity was found in cerebellar Purkinje cells and their dendritic processes, consistent with the findings of Pillot et al. [21] and Chazot et al. [22]. The cerebellum has been recognized as a region involved in sensory integration and pain processing, and neuroimaging studies have reported cerebellar alterations in patients with migraine [28, 29]. H3R expression in Purkinje cells may be relevant to the modulation of cerebellar neuronal activity, although its specific contribution to migraine remains unclear.

H3R was additionally detected in the thalamus, especially in the anteromedial nucleus. Previous studies have demonstrated H3R expression and receptor binding in several thalamic

regions [14, 20, 21]. The thalamus plays a role in sensory transmission and is a major component of the central trigeminovascular pathway. Although some differences in regional and cellular distribution were observed between studies, these may be due to differences in species and experimental methods.

Notably, the presence of H3R in the hypothalamus and brainstem is of interest, as these regions play important roles in the different phases of migraine attacks. Human imaging studies have demonstrated hypothalamic activity during the premonitory phase and changes in hypothalamic function in patients with migraine [30, 31]. Brainstem activation has also been reported during migraine attacks [32, 33]. In the present study, H3R immunoreactivity was observed in the supraoptic and suprachiasmatic nuclei of the hypothalamus, as well as in several pontine and medullary structures, including the medial vestibular nucleus (MVe). The presence of H3R in the MVe is of interest, as this nucleus plays a role in vestibular processing and may contribute to migraine-associated symptoms such as dizziness and vertigo, especially in vestibular migraine. Although these regions do not necessarily correspond to the specific areas activated during migraine attacks, our findings suggest that H3R may modulate the neuronal activity within hypothalamic and brainstem networks associated with migraine pathophysiology.

The presence of H3R in these regions is also supported by human PET imaging studies demonstrating H3R availability in the brain [34]. H3R acts mainly as an inhibitory auto-receptor and heteroreceptor that regulates the release of histamine and other neurotransmitters [11, 35]. However, the functional involvement of H3R in migraine remains to be established [7, 36].

H3R expression in the peripheral ganglia and its relationship with CGRP

The TG and upper cervical DRG provide sensory innervation to cranial structures, including the meninges and cerebral blood vessels, and are important components of the TVS [5, 37]. In the present study, H3R immunoreactivity was observed in the TG and DRG, with a similar staining pattern in neurons, SGCs and nerve fibers. Previous work by Cannon et al. [38] demonstrated H3R immunoreactivity in DRG neurons and peripheral sensory fibers, including CGRP-positive periarterial Aδ fibers. These findings are consistent with our observations and support the presence of H3R in peripheral sensory pathways.

An interesting finding was the expression of H3R in CGRP-positive trigeminal neurons. CGRP is an important neuropeptide in migraine pathophysiology and is involved in TVS [4, 5, 39]. In our study, H3R and CGRP were detected in the same small to medium-sized TG neurons and they were co-localized in the cytoplasm of neurons and in some C-fibers. Since H3R is known to regulate neurotransmitter release [35], its presence in CGRP-containing neurons supports the possibility that histaminergic signaling may influence trigeminal nociceptive activity. Whether H3R activation directly affects CGRP release remains to be investigated.

H3R immunoreactivity was also detected in the SPG, which is involved in cranial parasympathetic regulation and contributes to the trigeminal autonomic reflex. Parasympathetic pathways are associated with cranial autonomic symptoms during migraine and cluster headache [37, 40]. The presence of H3R in SPG neurons and fibers suggests that histaminergic signaling may influence parasympathetic activity, although its functional role in this ganglion is still unclear.

Our RT-qPCR results further demonstrated H3R mRNA expression in both the hypothalamus and TG, with significantly higher levels in the hypothalamus. This is in agreement with previous reports showing extensive H3R expression in the CNS, particularly in hypothalamic

regions [14, 20]. Together with the immunohistochemical findings, these results support the presence of H3R in both central and peripheral structures associated with migraine.

H3R in cerebral arteries

Another finding was the presence of H3R immunoreactivity in cerebral arteries, mainly localized in endothelial cells. Histamine is known to influence vascular function through different histamine receptors, while H3R is primarily recognized for its role in regulating neurotransmitter release [35]. Our findings suggest that H3R is present in the endothelial layer of cerebral arteries. Its possible contribution to endothelial signaling or the regulation of cerebrovascular function remains unclear and requires further investigation.

Limitations

This study has some limitations. First, the experiments were performed in rats, and further studies are needed to determine whether a similar H3R distribution is present in humans. Second, although three different H3R antibodies were examined, differences in staining intensity and subcellular localization were observed. In particular, the predominantly nuclear staining requires further validation. Finally, the present study focused on H3R distribution and did not investigate H3R function. Additional functional studies are therefore needed to clarify whether H3R regulates CGRP release, neuronal activity or vascular signaling in migraine-related structures.

Conclusion

The present study demonstrates widespread H3R immunoreactivity in central and peripheral structures associated with migraine, including several brain regions, sensory and parasympathetic ganglia and cerebral arteries. The expression of H3R in CGRP-positive trigeminal neurons is of particular interest and suggests a possible interaction between

histaminergic and CGRP-related signaling in the TVS. These findings provide an anatomical basis for further studies investigating the role of H3R in migraine pathophysiology.

References

1. Uthman OA. (2016) Global, regional, national incidence, prevalence and years lived with disability for 310 acute and chronic diseases and injuries 1990-2015: a systematic analysis for the Global Burden of Disease Study 2015. *Lancet*. 388(10053):1545-602.

2. Lipton RB, Bigal ME, Diamond M, Freitag F, Reed ML, Stewart WF. (2007) Migraine prevalence, disease burden, and the need for preventive therapy. *Neurology*. 68(5):343-9.

3. Steiner TJ, Stovner LJ. (2023) Global epidemiology of migraine and its implications for public health and health policy. *Nature Reviews Neurology*. 19(2):109-17.

4. Iyengar S, Ossipov MH, Johnson KW. (2017) The role of calcitonin gene–related peptide in peripheral and central pain mechanisms including migraine. *Pain*. 158(4):543-59.

5. Edvinsson L. (2017) T he T rigeminovascular P athway: R ole of CGRP and CGRP R eceptors in M igraine. *Headache: The Journal of Head and Face Pain*. 57:47-55.

6. Sgambellone S, Marri S, Masini E, Lucarini L. New insight in histamine functions. MDPI; 2022. p. 609.

7. Alstadhaug KB. (2014) Histamine in migraine and brain. *Headache: The Journal of Head and Face Pain*. 54(2):246-59.

8. Pickering GW, Hess W. (1932) Headache produced by histamine and its mechanism. *British Medical Journal*. 2(3754):1097.

9. DALSGAARD-NIELSEN T. (1945) Histaminhovedpine. *Ugeskrift for laeger*. 107:377.

10. Lassen LH, Thomsen LL, Olesen J. (1995) Histamine induces migraine via the H1-receptor. Support for the NO hypothesis of migraine. *Neuroreport*. 6(11):1475-9.

11. Arrang J-M, Garbarg M, Schwartz J-C. (1983) Auto-inhibition of brain histamine release mediated by a novel class (H3) of histamine receptor. *Nature*. 302(5911):832-7.

12. Esbenshade T, Browman K, Bitner R, Strakhova M, Cowart M, Brioni J. (2008) The histamine H3 receptor: an attractive target for the treatment of cognitive disorders. *British journal of pharmacology*. 154(6):1166-81.

13. Gemkow MJ, Davenport AJ, Harich S, Ellenbroek BA, Cesura A, Hallett D. (2009) The histamine H3 receptor as a therapeutic drug target for CNS disorders. *Drug discovery today*. 14(9-10):509-15.

14. Pollard H, Moreau J, Arrang J, Schwartz J. (1993) A detailed autoradiographic mapping of histamine H3 receptors in rat brain areas. *Neuroscience*. 52(1):169-89.

15. Lange IH, Maddahi A, Edvinsson L, Pellesi L. (2026) Migraine-inducing effects of pitolisant in women with migraine without aura: Protocol for a randomized, double-blind, placebo-controlled crossover trial. *Cephalalgia Reports*. 9:25158163261474461.

16. Hansen-Schwartz J, Hoel NL, Zhou M, Xu CB, Svendgaard NA, Edvinsson L. (2003) Subarachnoid hemorrhage enhances endothelin receptor expression and function in rat cerebral arteries. *Neurosurgery*. 52(5):1188-94; 94-5.

17. May A. (2017) Understanding migraine as a cycling brain syndrome: reviewing the evidence from functional imaging. *Neurological Sciences*. 38(Suppl 1):125-30.

18. Warfvinge K, Edvinsson L. (2019) Distribution of CGRP and CGRP receptor components in the rat brain. *Cephalalgia*. 39(3):342-53.

19. Raggi A, Leonardi M, Arruda M, Caponnetto V, Castaldo M, Coppola G, et al. (2024) Hallmarks of primary headache: part 1–migraine. *The journal of headache and pain*. 25(1):189.
20. Pillot C, Heron A, Cochois V, Tardivel-Lacombe J, Ligneau X, Schwartz J-C, et al. (2002) A detailed mapping of the histamine H3 receptor and its gene transcripts in rat brain. *Neuroscience*. 114(1):173-93.
21. Chazot PL, Hann V, Wilson C, Lees G, Thompson CL. (2001) Immunological identification of the mammalian H3 histamine receptor in the mouse brain. *Neuroreport*. 12(2):259-62.
22. Gao M, Ooms JF, Leurs R, Vischer HF. (2024) Histamine H3 receptor isoforms: insights from alternative splicing to functional complexity. *Biomolecules*. 14(7):761.
23. Martins D, Veronese M, van Wamelen D, Shan L, Howes O, Hampshire A, et al. (2026) Mapping histamine pathway networks in the human brain across cognition and psychiatric disorders. *Nature Mental Health*.1-13.
24. Welch K, Nagesh V, Aurora SK, Gelman N. (2001) Periaqueductal gray matter dysfunction in migraine: cause or the burden of illness? *Headache: The Journal of Head and Face Pain*. 41(7):629-37.
25. Vila-Pueyo M, Hoffmann J, Romero-Reyes M, Akerman S. (2019) Brain structure and function related to headache: Brainstem structure and function in headache. *Cephalalgia*. 39(13):1635-60.
26. Yoshida A, Moritani M, Nagase Y, Bae YC. (2017) Projection and synaptic connectivity of trigeminal mesencephalic nucleus neurons controlling jaw reflexes. *Journal of oral science*. 59(2):177-82.
27. Ono M, Ito T. (2015) Functional organization of the mammalian auditory midbrain. *The Journal of Physiological Sciences*. 65(6):499-506.
28. Mehnert J, May A. (2019) Functional and structural alterations in the migraine cerebellum. *Journal of Cerebral Blood Flow & Metabolism*. 39(4):730-9.
29. Qin Z, He X-W, Zhang J, Xu S, Li G-F, Su J, et al. (2019) Structural changes of cerebellum and brainstem in migraine without aura. *The journal of headache and pain*. 20(1):93.
30. Maniyar FH, Sprenger T, Monteith T, Schankin C, Goadsby PJ. (2014) Brain activations in the premonitory phase of nitroglycerin-triggered migraine attacks. *Brain*. 137(1):232-41.
31. Schulte LH, Allers A, May A. (2017) Hypothalamus as a mediator of chronic migraine: evidence from high-resolution fMRI. *Neurology*. 88(21):2011-6.
32. Weiller C, May A, Limmroth Va, Jüptner M, Kaube H, Schayck R, et al. (1995) Brain stem activation in spontaneous human migraine attacks. *Nature medicine*. 1(7):658-60.
33. Afridi S, Matharu M, Lee L, Kaube H, Friston K, Frackowiak R, et al. (2005) A PET study exploring the laterality of brainstem activation in migraine using glyceryl trinitrate. *Brain*. 128(4):932-9.
34. Arumuham A, Nour MM, Veronese M, Onwordi EC, Rabiner EA, Howes OD. (2023) The histamine system and cognitive function: An in vivo H3 receptor PET imaging study in healthy volunteers and patients with schizophrenia. *Journal of Psychopharmacology*. 37(10):1011-22.
35. Panula P, Chazot PL, Cowart M, Gutzmer R, Leurs R, Liu WL, et al. (2015) International union of basic and clinical pharmacology. XCVIII. Histamine receptors. *Pharmacological reviews*. 67(3):601-55.
36. Worm J, Falkenberg K, Olesen J. (2019) Histamine and migraine revisited: mechanisms and possible drug targets. *The journal of headache and pain*. 20(1):30.
37. Goadsby PJ, Holland PR, Martins-Oliveira M, Hoffmann J, Schankin C, Akerman S. (2017) Pathophysiology of migraine: a disorder of sensory processing. *Physiological reviews*.
38. Cannon KE, Chazot PL, Hann V, Shenton F, Hough LB, Rice FL. (2007) Immunohistochemical localization of histamine H3 receptors in rodent skin, dorsal root ganglia, superior cervical ganglia, and spinal cord: potential antinociceptive targets. *Pain*. 129(1-2):76-92.

39. Edvinsson L, Haanes KA, Warfvinge K, Krause DN. (2018) CGRP as the target of new migraine therapies—successful translation from bench to clinic. *Nature Reviews Neurology*. 14(6):338-50.
40. Hoffmann J, Baca SM, Akerman S. (2019) Neurovascular mechanisms of migraine and cluster headache. *Journal of Cerebral Blood Flow & Metabolism*. 39(4):573-94.
41. Paxinos G, Watson C. The rat brain in stereotaxic coordinates, Ed 6. Amsterdam: Academic. Elsevier; 2007.

Abbreviations

AON: anterior olfactory nucleus; AOV: anterior olfactory area; AOP: anterior olfactory peduncle; AM: anterior medial thalamic region; BA: basilar artery; BSA: Bovine serum albumin; CGRP: Calcitonin gene-related peptide; CNS: Central nervous system; cDNA: Complementary DNA; CA1: field CA1 of the hippocampus; CA2: field CA2 of the hippocampus; CA3: field CA3 of the hippocampus; Cb: Cerebellum; cu: cuneate nucleus; DG: dentate gyrus; DRG: dorsal root ganglion; DCIC: Dorsal cortex of Inferior colliculus; DAPI: 4', 6-diamidino-2-phenylindole; DNA: Deoxyribonucleic acid; Ecu: external cuneate nucleus; IC: Inferior colliculus; GAPDH: Glyceraldehyde-3-phosphate dehydrogenase; Gran layer: Cerebellar granular layer; HT: Hypothalamus; H3R: Histamin three receptor; lfp: longitudinal fasciculus pons; Mve: Middle vestibular nucleus; Me5: Mesencephalic trigeminal nucleus; Med: Medial cerebellar nu; Mol layer: Cerebellar molecular layer; mRNA: Messenger RNA; OX: optic chiasm; PBS: Phosphate buffer saline; PBS-T: Phosphate buffer saline-TritonX; PF: Paraformaldehyde; Pc: Purkinje cell; PF: Paraformaldehyde; Pn: Pontine nuclei; PnO: pontine reticular nucleus; PVA: Paraventricular thalamic nu; PVN: Paraventricular hypothalamic nu; PAG: periaqueductal gray; RNA:

Ribonucleic acid; RT-qPCR: Real-time quantitative Polymerase Chain Reaction; SGC: Satellite glial cell; SPG: Sphenopalatine ganglion; SMC: smooth muscle cell; SON: Supraoptic nucleus; SCh: suprachiasmatic; SCN: suprachiasmatic nucleus; Sp5: Spinal trigeminal nu; Sol: solitary tract; tfp: transverse fibers pons; TVS:Trigeminovascular system; TG: trigeminal ganglion; tz : trapezoid body; Tz: nucleus of trapezoid body.

Declarations

Ethics Approval and consent to participate

Consent for publication

All authors have agreed to publish the data in this manuscript.

Availability of data and materials

The datasets generated during and/or analyzed during the current study are available from the corresponding author on reasonable request.

Competing Interests

The authors declare no potential conflicts of interest with respect to the research, authorship, and/or publication of this article.

Funding

This work was supported by Pfizer and Lundbeck Foundations. The funding organizations had no role in study design, data collection and analysis, decision to publish, or preparation of the manuscript.

Author contributions

AM, LP, and LE designed the study, AM performed immunohistochemistry and RT-qPCR and analyzed the data. LE and AM provided tools and reagents. All authors wrote the manuscript, read and commented on the final manuscript

Figure legends

Fig. 1. Expression of H3R gene in rat TG and hypothalamus. H3R gene was expressed in both TG and HT, however the mRNA level for H3R was significantly higher in HT compared to the TG. Expression was normalized to housekeeping gene GAPDH. Data are presented as mean ± SEM, statistical significance indicate as **$p < 0.01$, and *n=8.*

Fig.2. Pre-absorption control with blocking peptide. A. Image from anti rat H3R antibody **B.** Pre-absorption with H3R antibody and its respective blocking peptide. Arrows in A indicate positive neurons and fibers. No positive immunoreactivity is observed in the neurons or fibers when the blocking peptide is used.

Fig. 3. H3R immunoreactivity in the TG. A. H3R immunoreactivity was observed in the nuclei of TG neurons (thick arrows), in SGCs (thin arrows) and in fibers (arrow heads). **B.** Higher magnification of A with DAPI staining**.** Blue color represents nuclei staining with DAPI.

Fig. 4. H3R immunoreactivity in SPG, TG, and DRG. A. H3R immunoreactivity in SPG, **B.** H3R immunoreactivity in TG, and **C.** H3R immunoreactivity in DRG. H3R expression in

the SPG and DRG was similar as its expression in TG, with staining detected in the nuclei of neurons, SGCs and fibers (presumably, Aδ-fibers).

Fig. 5. Double immunofluorescence staining of H3R with CGRP in the TG. A: H3R (green color) was expressed in the nuclei of TG neurons (thick arrows). **B.** CGRP (red color) was expressed in the cytoplasm of TG neurons (thick arrows) and in C- fibers (arrowhead). **C.** The merged image shows that H3R was co-expressed with CGRP in same small to medium-sized neurons. Blue represents nuclei staining with DAPI.

Fig. 6. Distribution of H3R immunoreactivity in the rat brain and its relationship to CGRP distribution and migraine-related regions. Schematic representation of the regional distribution of H3R immunoreactivity (purple) in a sagittal section of the rat brain compared with the distribution of CGRP (green) and brain regions implicated in migraine pathophysiology (red). Anatomical structures were identified using the sixth edition of *The Rat Brain in Stereotaxic Coordinates* by Paxinos and Watson [41].

Fig.7. H3R immunoreactivity in the pons and medulla regions. A & B. H3R expression was observed in the pontine nuclei (Pn), with strong staining in neuronal cell bodies (arrows) and nerve fibers (arrowheads). H3R immunoreactivity was also observed in the transverse fibers (tfp) and longitudinal fasciculus of the pons (lfp). **B**. Higher magnification image of the region shown in A. **C**. H3R immunoreactivity was observed in the neuronal cell bodies (arrows) and in the fibres (arrowheads) in the trapezoid body (TZ). **D.** H3R immunoreactivity in the inferior olivary (IO) of the medulla oblongata. H3R immunoreactivity was detected in neuronal cell bodies (arrow) and fibers (arrowhead). Cell nuclei are stained with DAPI (blue).

Fig. 8. H3R immunoreactivity in the medulla oblongata. A. Low magnification image shows the distribution of H3R in the external cuneate nucleus (Ecu), cuneate nucleus (cu), and solitary nucleus (Sol). **B.** Higher magnification image showing H3R immunoreactivity in

the cuneate and solitary nuclei. **C**. Strong H3R immunoreactivity was observed in neuronal cell bodies and nerve fibers forming a dense network throughout the solitary region. **D.** H3R immunoreactivity in the medial vestibular nucleus (MVe), with intense staining in neuronal cell bodies (arrows). Cb, cerebellum.

Fig.9. H3R immunoreactivity in the cerebellum. A. H3R immunoreactivity was observed in Purkinje cell bodies (Pc, arrowhead) and their dendritic processes (large arrow) extending into the molecular layer. Small arrows indicate H3R-positive nuclei in the molecular layer. **B.** Higher magnification image shows H3R immunoreactivity in both cytoplasm and nuclei of Purkinje cell bodies (arrowhead), as well as in the dendritic branches (large arrow). Blue represents nuclei staining with DAPI.

Fig.10. H3R immunoreactivity in the cerebral cortex. Representative immunofluorescence images showing H3R expression in the cerebral cortex at different magnifications (A-C). **A.** H3R immunoreactivity was observed in neuronal cell bodies (arrows) and nerve fibers (arrowheads) throughout most cortical layers (I-V). **B &C.** Higher magnification images showing strong H3R immunoreactivity localized in both cytoplasm and nuclei of neuronal cell bodies (arrows) and nerve fibers (arrowheads). Cell nuclei are stained with DAPI (blue).

Fig.11. H3R immunoreactivity in the midbrain. H3R immunoreactivity in the (**A)** dorsal cortex of the inferior colliculus (DCIC), **(B)** periaqueductal gray (PAG), and **(C)** mesencephalic trigeminal nucleus (Me5). H3R immunoreactivity was observed in neuronal cell bodies (arrows) and nerve fibers (arrowheads) in all three regions. Cell nuclei are stained with DAPI (blue).

Fig.12. H3R immunoreactivity in the hippocampus. A. H3R expression was observed in the hippocampus, including the dentate gyrus (DG) and CA1- CA2 regions. **B &C.** Higher magnification images showing strong H3R immunoreactivity in cells of the dentate gyrus and neuronal cell bodies in the CA1 region (arrows).

Fig.13. H3R immunoreactivity in the hypothalamus and thalamus. Representative immunofluorescence images showing H3R expression in different regions of the hypothalamus and thalamus. **A.** H3R immunoreactivity in the supraoptic nucleus (SO) adjacent to the optic chiasm (OX). **B**. H3R immunoreactivity in the suprachiasmatic nucleus (Sch). **C.** H3R immunoreactivity in the anteromedial thalamic nucleus (AM). Strong H3R immunoreactivity was observed in neuronal cell bodies, predominantly in the nuclei (arrows) in all three regions.

Fig.14. H3R immunoreactivity in the olfactory region. A. H3R expressions in the ventral (AOV) and posterior (AOP) parts of the anterior olfactory nucleus. The H3R immunoreactivity was observed in neuronal cell bodies (arrowheads) and fibers (arrows). **B**. Higher magnification view of the region shown in A. Blue represents cell nuclei staining with DAPI.

Fig.15. H3R immunoreactivity in the wall of cerebral arteries. A & B. H3R immunoreactivity was mainly observed in the endothelium (arrowhead) and in some extent in the smooth muscle cells (thick arrows). Blue represents nuclei staining with DAPI.

Supplementary fig.1. H3R immunoreactivity in the TG. A & B. H3R immunoreactivity was observed in neuronal cell bodies, mostly in the nuclei (thick arrows), with some cytoplasmic staining (arrowheads), as well as in satellite glial cells (asterisks) and in fibers. Blue represents nuclei staining with DAPI in image B.

Supplementary fig.2. Double immunofluorescence staining of H3R and CGRP in the TG. A. H3R immunoreactivity (green) was detected in both cytoplasm and nuclei of TG neurons and in fibers. **B.** CGRP immunoreactivity (red) in the cytoplasm of neuronal cell bodies and c-fibers. **C.** Merged image showing co-localization of H3R and CGRP in the cytoplasm of some neuronal cell bodies (orange, arrows) and in a few thin fibers (arrowhead). Cell nuclei are stained with DAPI (blue).

Supplementary Files

This is a list of supplementary files associated with this preprint. Click to download.

- supplementaryfig.1final.tif
- Supplementaryfig.2final.tif